MEDIUM-LATITUDE VLF/ELF EMISSIONS AS DEDUCED FROM THE MULTI-STATIONED DIRECTION FINDING MEASUREMENTS

Masashi HAYAKAWA, Yoshihito TANAKA, Akira IWAI, Jinsuke OHTSU, Mizuo KASHIWAGI and Toshimi OKADA

Research Institute of Atmospherics, Nagoya University, 13, Honohara 3-chome, Toyokawa 442

Abstract: Some early results are presented on medium-latitude VLF/ELF emissions observed by the simultaneous measurements at the two stations in Europe during November 1978 through January 1979. The main aim of the present research is the adoption of two different kinds of direction finding systems; (i) a field-analysis direction finding, and (ii) a goniometer network, which has enabled us to locate the ionospheric exit points of different kinds of VLF/ELF emissions over a wide range in L values. The VLF/ELF emissions observed are found to be classified into four major categories; (1) plasmapause-associated VLF emissions, (2) VLF hiss in the electron slot region, (3) periodic hiss emissions, and (4) periodic VLF emissions triggered by the hiss band. The characteristics of one example from each category are described, and the mechanisms of their generation and propagation will be studied in the future.

1. Introduction

Recent satellite and ground studies have yielded that the medium-latitude VLF emission is not the consequence of the earth-ionosphere waveguide propagation of auroral hiss, but it has features distinct from auroral hiss such as a strong correlation with geomagnetic disturbances and a band-limitation in the frequency spectrum (HAYAKAWA *et al.*, 1975). Furthermore, those storm-time VLF emissions are likely to be generated around the plasmapause due to the cyclotron instability by the ring current electrons (BULLOUGH *et al.*, 1969; RYCROFT, 1972; TANAKA *et al.*, 1974; FOSTER and ROSENBERG, 1976; HAYAKAWA *et al.*, 1977).

In addition to the above-mentioned storm-time VLF emissions occurring just around the plasmapause, it seems likely that there are many other types of VLF emissions. So many problems are still unsolved in various types of mid-latitude VLF emissions. We can show some of them; (1) The global behavior of the occurrence of storm-associated VLF/ELF emissions in LT (local time)—L plot during the progress of the storm is not clearly established. (2) What is the controlling factor for the band-limitation in the frequency spectra? (3) Chorus tends to be generated outside the plasmapause, while hiss within the plasmapause. What is the essential

difference between the two, or is hiss merely the result of a sufficient density of overlapping chorus? (4) What are the characteristics of other discrete emissions?

In order to improve understanding of those points, we have carried out the studies using ground stations located at invariant latitudes of ~40° to 60°. The major object of our experiment was to make full use of the direction finding (DF) of two different systems at multiple stations. The present VLF project consisted of the campaign during three years, but some early results on VLF/ELF emissions are presented from the final year's measurement (November 1978 to January 1979).

2. Observing Stations and VLF Equipments

Table 1 shows the names and coordinates of the three stations where the simultaneous measurements were made, and Fig. 1 illustrates the locations of the two European stations. The L values of Brorfelde and Chambon-la-Foret are approximately 3.0 and 2.0, respectively, being lower than the average plasmapause location of ~4.0. However, the use of the two different kinds of DF enables us to locate the ionospheric exit points of emissions at L value up to or more than 4.0. The time delay in the temporal evolutions of VLF emissions at the European stations and at Moshiri would be useful for the study of the drift velocity of energetic electrons responsible for the VLF emissions.

There are three major items of the measurement; (1) continuous recording of the intensity of hiss-type emissions at 5 and 3 kHz by means of hiss recorders, (2) continuous recording of the arrival angle and polarization of VLF emissions at 5 kHz, and (3) synoptic two-minutes sampling measurement of wide-band VLF signals (goniometer measurement).

Two different kinds of DF systems have been adopted, (i) a field-analysis DF system (OKADA *et al.*, 1981), and (ii) a goniometer network (HAYAKAWA *et al.*, 1981). Some parts of the former system are described here. The wave is assumed to be incident on the direction finder with an incident angle (i) from the zenith and an azimuthal angle (θ) measured clockwise from the north, and the wave polarization in the wavefront is given by $P=H_{\parallel}/H_{\perp}\exp(-jQ)=x-jy$ (*e.g.* right-handed circular polarization; $x=0$, $y=-1$), where $H_{\parallel}$ and $H_{\perp}$ are the amplitudes of parallel and perpendicular magnetic fields to the plane of wave incidence, and Q is the phase dif-

Table 1. Names and coordinates of the VLF stations.

Station name	Geographic		Geomagnetic		L-value
	latitude	longitude	latitude	longitude	
Brorfelde (Denmark)	55°38′N	11°40′E	55.7°N	97.8°E	2.9
Chambon-1a-Foret (France)	48°01′N	2°16′E	50.4°N	84.6°E	1.9
Moshiri (Japan)	44°22′N	142°16′E	34.4°N	207.0°E	1.6

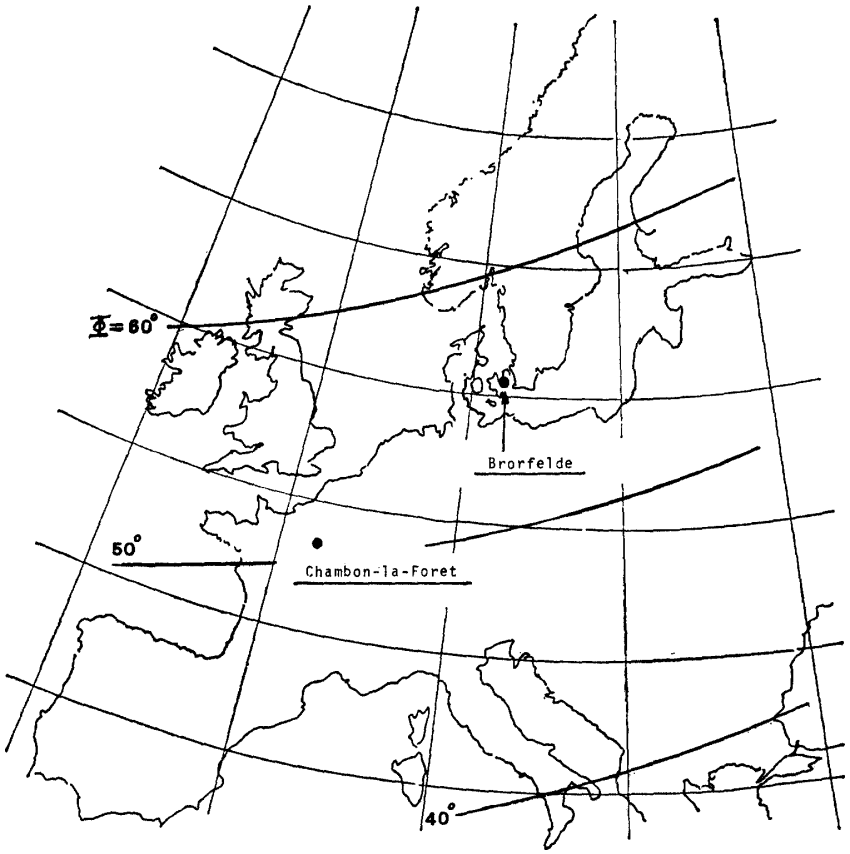

Fig. 1. Location of the two European VLF stations of Brorfelde and Chambon-la-Foret.

ference between the both fields. The correlations for the following combinations among the v_x, v_y (horizontal magnetic field components) and v_z (vertical electric field component) signals at 5 kHz yield the three signals of α, β and γ (OKADA *et al.*, 1981).

α=low freq. comp. $[v_y \cdot v_x(-90°)] = 1/2\ A^2\ y \cos i$

β=low freq. comp. $[v_z \cdot v_y(-90°)] = 1/2\ A^2\ y\ (\cos i \sin i) \sin \theta$

γ=low freq. comp. $[v_z \cdot v_x(-90°)] = -1/2\ A^2\ y\ (\cos i \sin i) \cos \theta$

where A is the amplitude of the TM mode component of the incident wave, and $(-90°)$ indicates a lag in phase by 90° behind the corresponding signal.

The above field-analysis DF has a relatively small covering range, a few hundred kilometers from the station; in other words, it is effective for elliptically polarized waves having emerged from the ionosphere within that range. However, it is of no use for the VLF signals with a small elevation angle or with a small polarization such as having propagated over great distances in the earth-ionosphere waveguide after exiting from the ionosphere. To be very effective for this situation, there exists another DF system, or the goniometer network (HAYAKAWA *et al.*, 1981).

By making use of the two DF systems which are complementary with each other, the triangulation by the two goniometers and a combination of the field-analysis DF with the goniometer enables us to locate the ionospheric exit points of VLF signals in a wide region of L value. Further details will be published elsewhere on the generation and propagation mechanisms of each category of VLF/ELF emissions.

3. Observation of VLF Emissions

During the final year's period of about three months we have identified about twenty emission events at Brorfelde, and about ten events at Chambon. The results of analyses have yielded that the VLF emissions tend to take place in the pre-midnight (22–23 LT) and in the dawn (06–07 LT) sectors. The observed mid-latitude emissions may be classified into several different categories; (1) plasmapause-associated VLF emissions, (2) VLF hiss in the electron slot region, (3) periodic hiss emissions, and (4) periodic VLF emissions triggered by the hiss band. In what follows, we describe the characteristics for one example from each category.

3.1. Plasmapause-associated VLF hiss

3.1.1. Direction finding results and frequency spectra

We show one example of VLF emission occurring during dawn times on 20 December 1978. Fig. 2 presents the temporal evolution of VLF emissions (5 kHz) during 07–08 LT and their direction finding results. The temporal variations at Brorfelde and at Chambon have shown a very good similarity with each other, indicating that the emission events at both stations originated in a single source. The peak power at Brorfelde is more enhanced than that at Chambon. Corresponding to the variation in power flux at Brorfelde, we find very remarkable variations in the outputs from α, β and γ. The movement of the ionospheric exit points is given in a polar plot between the second and third panels in Fig. 2, indicating that the exit points for this emission event have shifted from the southeast of the station, overhead it and then to the northwest of it, but relatively close to the station. Along with the three other examples for the plasmapause-associated VLF emissions, the field-analysis DF has shown clear variations in α, β, and γ at Brorfelde, this being apparently indicative that the exit points are relatively localized.

On the other hand, we find insignificant outputs from α, β and γ at Chambon, although we confirm that the direction finder is operating very well and we have a sufficient S/N ratio for this event. Such insignificant outputs from α, β and γ at Chambon are found to be valid for other events of plasmapause-associated VLF emissions, and this seems to be physically significant. The zero outputs for α, β and γ can only be expected either by the linear polarization ($y \cong 0$) or by the horizontal incidence ($i \cong 90°$). If we assume that the horizontal incidence of emissions exited from the ionosphere at a single localized region, followed by the earth-ionosphere

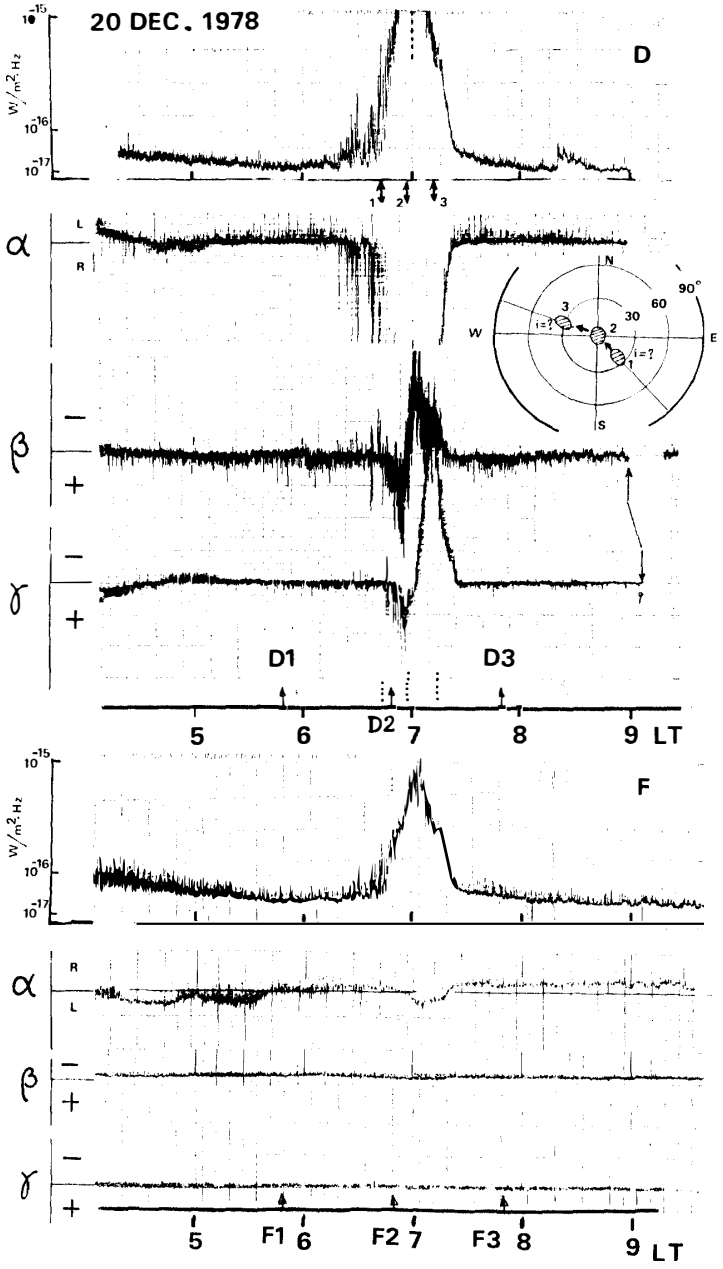

Fig. 2. The temporal evolution of the power flux at 5 kHz (top), and the corresponding direction finding results (α, β and γ) (second, third and fourth panels) on 20 December 1978. The above four panels refer to Brorfelde, and other four panels are from Chambon. The movement of exit points measured at Brorfelde is summarized in the polar plot, in which the distance of each dot representing the exit region from the origin means the incident angle (i) and the azimuthal angle (θ) is easily read. The numeric beside each dot corresponds to the time given below the abscissa of the variation of power flux.

waveguide, we would expect a well-defined amplitude-modulation in the goniometer output, as will be discussed for the VLF hiss in the electron slot in Subsection 3.2. In contradiction to this expectation, the goniometer at Chambon has indicated no amplitude modulation. In conclusion, the experimental result at Chambon can be reasonably interpreted in terms of the nature of the averaged linear polarization of VLF emissions. That is, the power flux at Chambon is considered to be composed of the emission exiting mainly from the two exit regions; one is near Brorfelde, having propagated in the waveguide over about one thousand kilometers, and the other emerged from the ionosphere near Chambon. In this case the emission of the former with nearly linear polarization as the consequence of the waveguide propagation and the emission of the latter with elliptical polarization are added to each other with unknown phase relationship, enabling us to expect, on the average, a linear polarization (TANAKA *et al.*, 1976). This model of the addition of more than two major exit

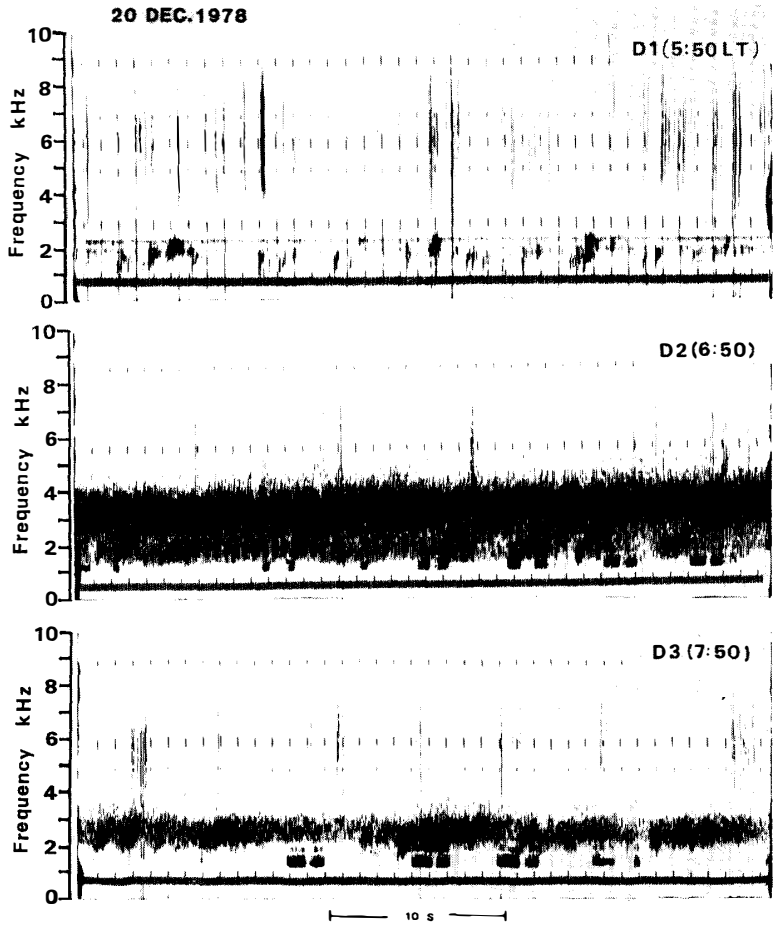

Fig. 3. Variation of frequency spectra of VLF emissions on 20 December 1978. The times of D1, D2 and D3 are given on the time axis of Fig. 2. D indicates the Danish result at Brorfelde, while F indicates the French result at Chambon.

points is additionally supported by the absence of amplitude modulation in the goniometer output at Chambon.

We now examine the variations in dynamic spectra for this emission event. Fig. 3 shows dynamic spectra of VLF emissions at Brorfelde during three time windows (D1 (0550 LT), D2 (0650) and D3 (0750)). During the D1 phase we observe no hiss activity, but we find bursts of chorus or riser emissions in the ELF band (1.0–2.5 kHz). During the D2 period there appears a band-limited hiss band of 3.0–4.5 kHz above the discrete emission band (1.0–2.5 kHz). Since the power flux at 5 kHz shows a maximum between the D1 and D2 periods, we might expect that the uppermost frequency of the hiss band during that time has extended to higher frequencies more than 5 kHz. Then during the D3 period when we have no activity at 5 kHz, the spectrogram has yielded band-limited ELF hiss emissions at 2–3 kHz including some chorus, and the lower frequency cutoff seems to remain approximately unchanged at around 2 kHz. Since no spectrograms are shown for Chambon, we give a brief description on the spectra there. During the F1 period corresponding to D1, no emission is present at Chambon, while exactly the same spectrum is confirmed for the F2 period, and a slightly wider spectrum is observed for the F3 period.

3.1.2. Association with geomagnetic disturbances and the generation of emissions

An association with substorm has been examined in Fig. 4, which shows the temporal variations of the magnetic field (X-component) at Kiruna (geomag. lat. 65°N) and of the Kp index. Onsets of the substorms are designated by arrows, and the period of occurrence of VLF emission is also given. The emission is associated with either one of the two successive substorms in the night of 19/20 December.

According to FOSTER and ROSENBERG (1976) and HAYAKAWA *et al.* (1977), the generation region of VLF emissions associated with geomagnetic disturbances is likely to be just around the plasmapause; hiss emissions inside the plasmapause, while chorus outside the plasmapause. The study for the present and other events

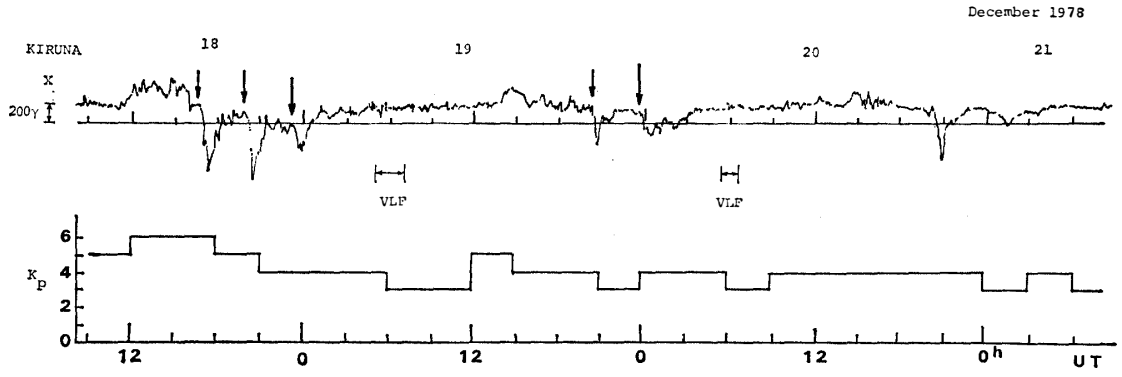

Fig. 4. The temporal variations of the magnetic field (X-component) at Kiruna and of Kp index during 18–21 December 1978 in which two dawn VLF emissions are observed.

have found that the emissions of hiss-type associated with geomagnetic disturbances are distributed very widely in latitude, having been received from the plasmapause latitude down to $L\sim2.0$, corresponding to the latitude of Chambon.

The plasmapause location can be estimated by using the experimental formula by CARPENTER and PARK (1973) for the dawn sector, and assuming the wave generation at the plasmapause ($L_{pp}=3.35$), we estimate the ratio of $f/f_c=0.14-0.20$ where f is the emission frequency and f_c the equatorial cyclotron frequency. The electron cyclotron instability seems to be the generation mechanism of VLF emissions, and the parallel energy of resonant electrons responsible for the wave generation is estimated (RYCROFT, 1972) to be $W_{\parallel}=15-8$ keV at the plasmapause. In the calculation we have used the electron density profile from ANGERAMI and CARPENTER (1966) and MATHUR *et al.* (1972).

Detailed investigation of the generation and propagation mechanisms will be published elsewhere in the future.

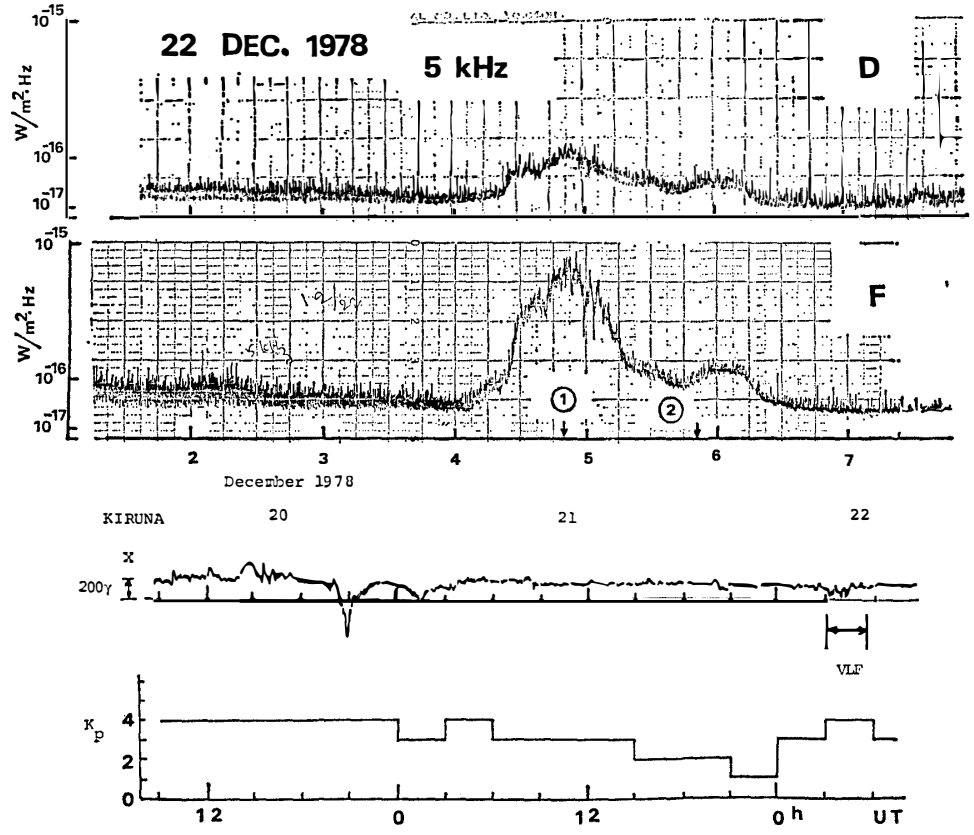

Fig. 5. The temporal variations of hiss power flux at 5 kHz at Brorfelde and at Chambon on 22 December 1978 (upper panel) and the corresponding temporal variation of magnetic field (X-component) at Kiruna during 20–22 December (lower panel).

3.2. *VLF hiss in the electron slot region; Direction finding results and frequency spectra*

We show an example of VLF hiss identified to occur in the electron slot region ($2<L<3.5$). This was the only one during the final year's campaign. Fig. 5 illustrates the temporal evolutions of power flux at 5 kHz at Brorfelde and Chambon

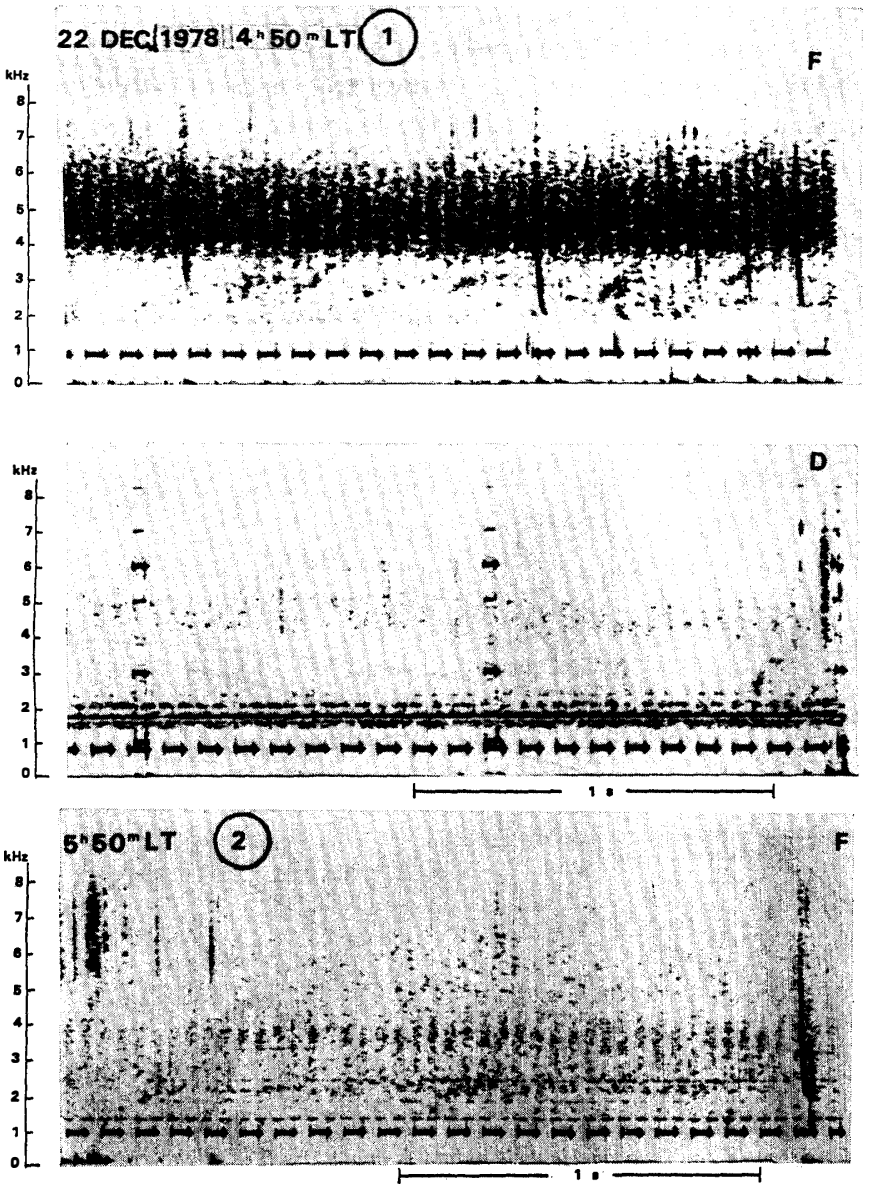

Fig. 6. The goniometer outputs for the emission event for Chambon (F) and for Brorfelde (D) indicating well-defined amplitude modulations at 0450 LT (upper two panels). The bottom panel refers to the goniometer output from Chambon (F) one hour later (0550 LT).

(upper panel) and the geomagnetic activity (lower panel). It is seen that the power flux is more enhanced at Chambon than at Brorfelde. The field-analysis DF data are found to be unavailable for this event, but we are successful in the triangulation location of the exit points of emissions based on the goniometer data. Spectrograms of wide-band output from the goniometer are illustrated in Fig. 6 at Chambon (upper panel) and at Brorfelde (lower one) at 0450 LT when we observed the maximum intensity at both stations and the one at Chambon one hour later (bottom panel). At 0450 LT the emission is of hiss type with a narrow band of 4–6 kHz, and one hour later we observed weak hiss emissions at lower frequencies (3–4 kHz).

At the time of maximum intensity, the ionospheric exit point of narrow band VLF hiss (4–6 kHz) is fixed in Fig. 7 in which circled dot (⊙) indicates the exit point determined by the mean values of azimuths measured from the two stations, and the shaded region resulted from the measuring errors at the two stations. The exit point denoted by circled dot (⊙) is found to have an L value of 2.2, just in the electron slot region ($2<L<3.5$), where the VLF emissions may play an important role in the

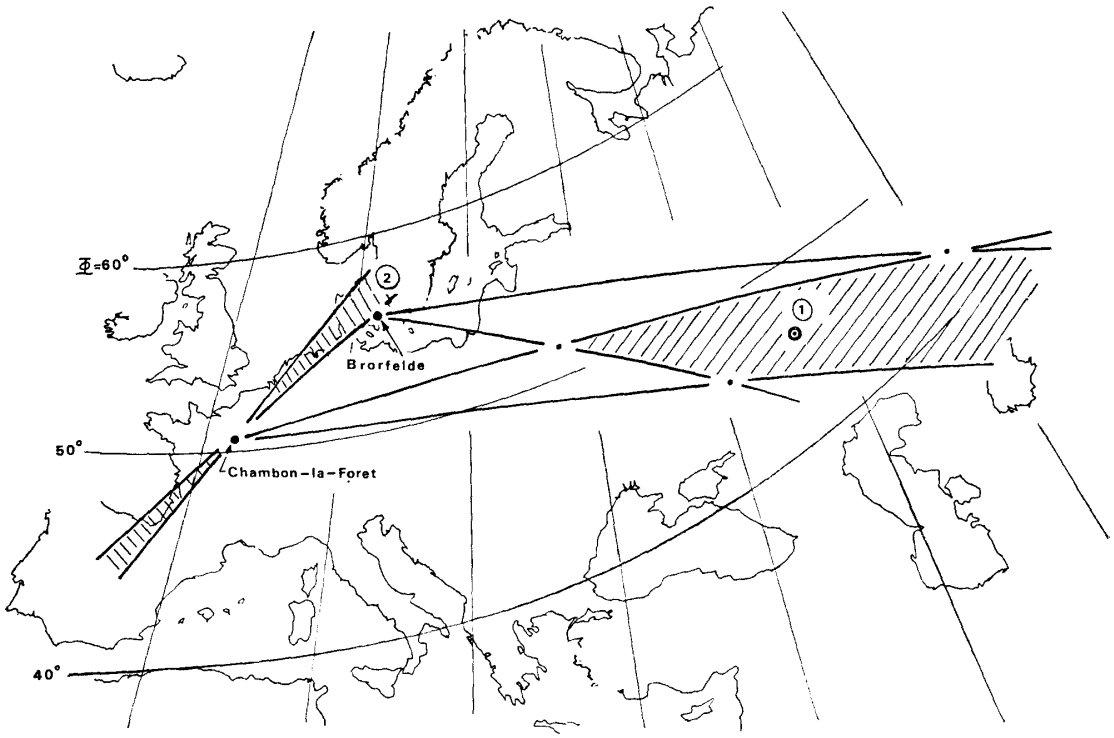

Fig. 7. Location of the ionospheric exit points (denoted by ①) of the emissions at 0450 LT. ① is determined by the triangulation by means of the mean azimuths from the two stations. The hatched region is the possible region taking into account the errors in azimuth measurement at both stations. During the interval (0550 LT) denoted by ②, the azimuth measurement at Chambon is only available, and the exit points must lie in the shaded region.

depletion of energetic electrons. Hence, this hiss emission has exited from the ionosphere at a very localized region, and followed by the earth-ionosphere waveguide over a few thousand kilometers, then received simultaneously at the two stations. One hour later (0550 LT) the sonagram has indicated the shifting of frequency band to lower frequencies (3–4 kHz). Since the power flux at Brorfelde is very weak, being unables to obtain clear amplitude modulation in the goniometer output, the result of the azimuth measurement at Chambon is illustrated in Fig. 7. The exit point of emissions at 0550 LT seems to be located much nearer to both stations than that at 0450 LT. The exit point of emissions at 0550 LT is seen to have shifted westwards from the region in the east at a speed of a few thousand kilometers per hour (or ~830 m/s). The spectra of these VLF hiss emissions are found to be very similar to those of plasmapause-associated VLF hiss, and it is difficult for us to distinguish between the two types of hiss emissions by means of frequency spectra alone. Although the plasmapause-associated VLF emissions have a strong correlation with geomagnetic substorms or storms, the correlation of this emission with remarkable geomagnetic disturbances is unclear at the present, but it seems that this emission event may have an association with the fluctuation of the magnetic field during 02–05 UT, being simultaneous with the emission occurrence.

3.3. Periodic hiss emissions

3.3.1. Direction finding results and frequency spectra

Very distinct periodic emissions have been observed at midnight of 3/4 November 1978. The field-analysis DF results at Brorfelde and at Chambon are presented in Fig. 8, and Fig. 9 indicates the temporal movement of the ionospheric exit points of those emissions, in which the exit points are determined at several specific times denoted by 1 to 6 during the course of the event. Fig. 10 shows the temporal variations of dynamic spectra of VLF emissions for the selected five time windows (D1 to D5). The DF result at Brorfelde in Fig. 9 indicates that the exit points have shown no systematic temporal and spatial movement, and the center of them is located approximately ~100 km south of the station. The region of the exit points is found to be distributed within a diameter of about 150 km, being very localised. Quite different from the cases for the plasmapause-associated VLF emissions, the DF result at Chambon has shown a significant variation. The result is available only for the time 4, but it indicates the azimuthal direction toward Brorfelde, and hence the direction finder at Chambon was looking at the exit region determined by the finder at Brorfelde.

It is interesting to examine the variation of spectrograms. During the D1 phase, we observe periodic emissions with a shape of knife head. The period does not seem to vary with frequency (T= 2.38–2.50 s), and these periodic emissions are 'non-dispersive'. A component of the periodic emissions is a burst of hiss emission with decreasing frequency with time in the frequency range between 6 and 3.5 kHz. Above

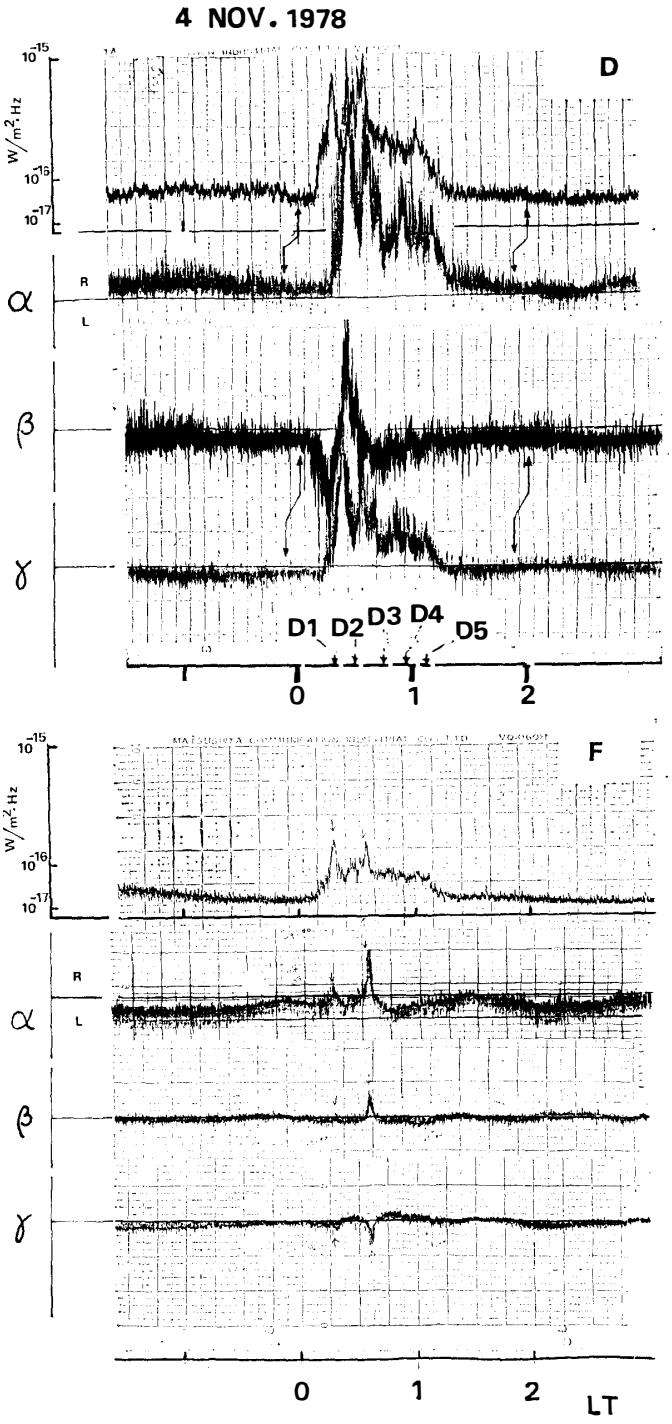

Fig. 8. The variations of power flux at 5 kHz and of the corresponding DF results at Brorfelde (D) (upper four panels) on 4 November, 1978. The lower four panels refer to Chambon (F).

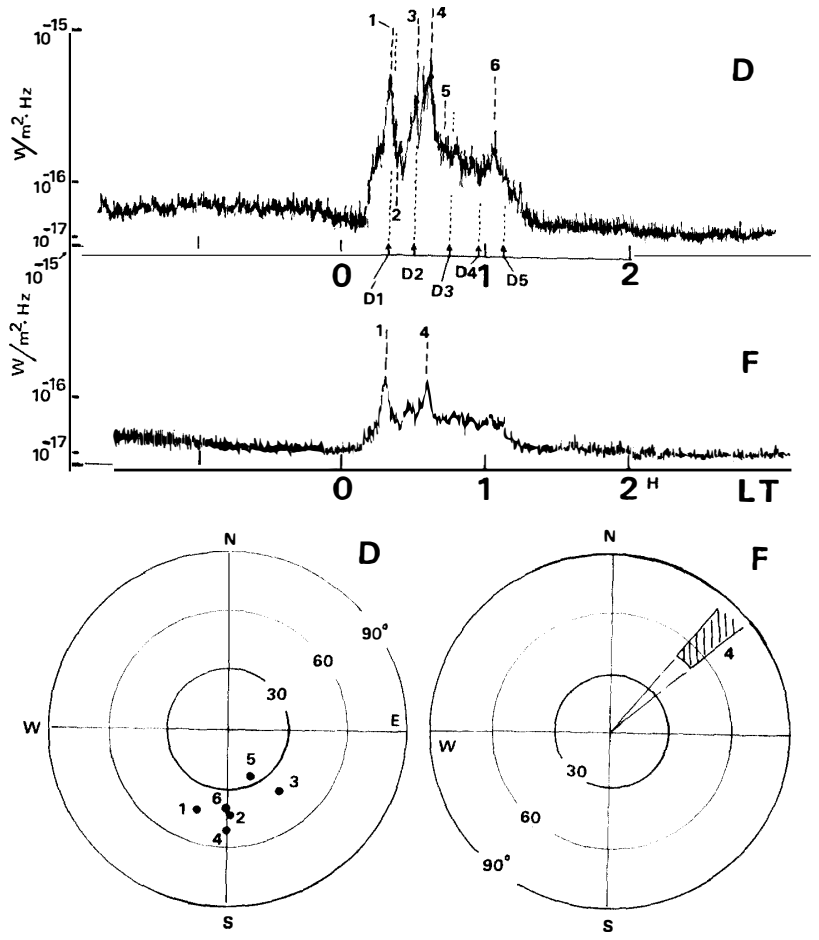

Fig. 9. The movement of ionospheric exit points of VLF emissions determined by means of α, β and γ. The number in the polar plot corresponds to the numeric in the variation of power flux. The error in the measurement of incident and azimuthal angles is about 10° and 15°, respectively.

the knife-head shaped periodic emissions, on the right in D1, are superimposed two series of periodic emissions (hiss bursts) designated by triangles (▼) and arrows (↓). So the observed periodic emissions may be called 'multi-phase (three phase)' periodic emissions. During the D2 period the upper frequency limit of the non-dispersive periodic emissions has extended upwards to ~6.6 kHz. During the D3 phase it is not clear whether the relatively weak periodic hiss bursts in 5.5 to 6.5 kHz (phase 1) and the dispersive periodic hiss bursts (phase 2) in the lower frequency below 5.5 kHz showing the temporal frequency decrease are the continuation of each other. Additionally, there is a third periodic emission of hiss burst in 3.0–4.0 kHz (phase 3). During the D4 period we observe that the periodic emissions have changed from non-dispersive to dispersive in the frequency range from 4 to 7 kHz. The period at

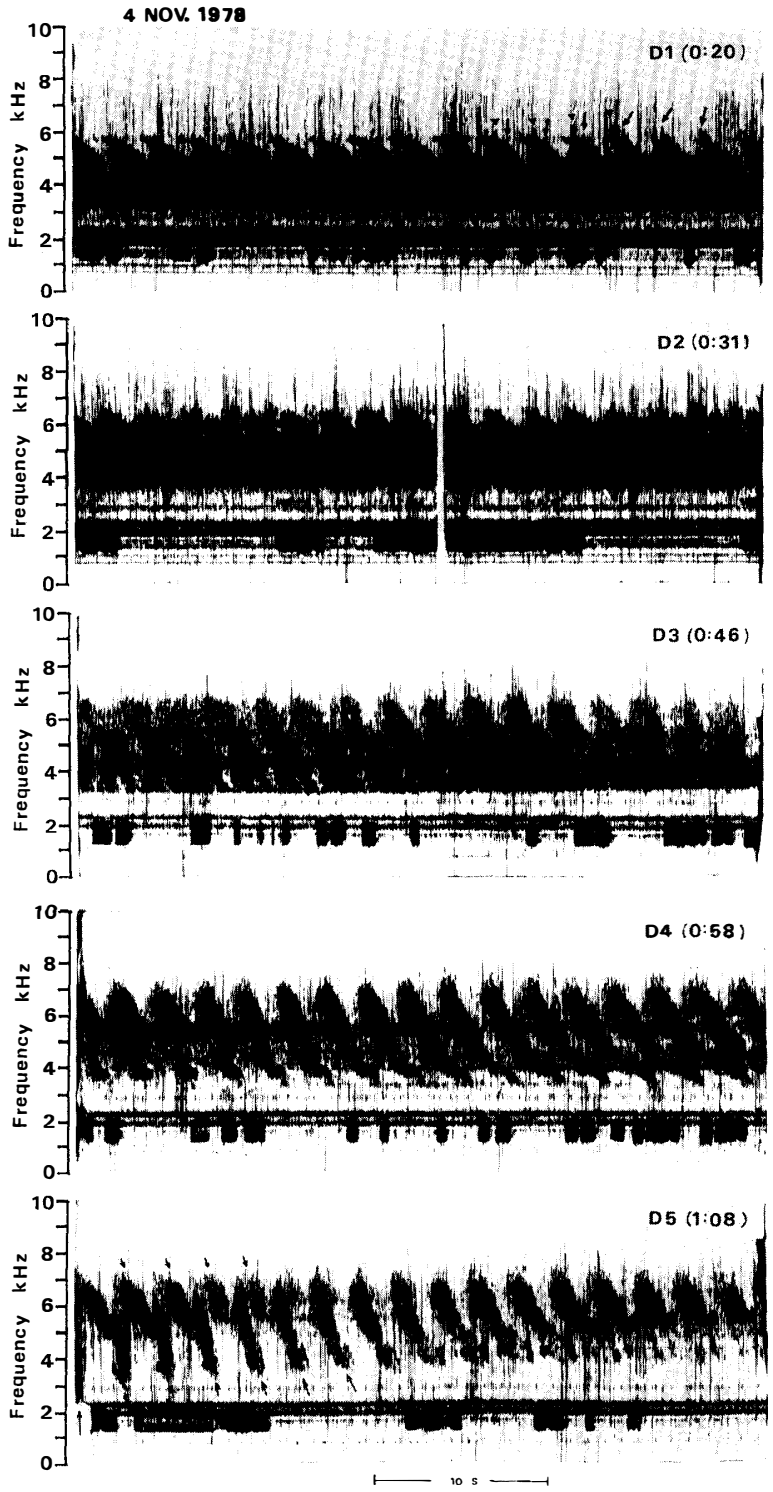

Fig. 10. The temporal variation of frequency spectra of periodic emissions for five time windows (D1 to D5). D indicates the result from Brorfelde.

7 kHz is 2.38 s, while it is 2.60 s at 4 kHz. At a frequency below 4 kHz there are series of hiss blobs which are accompanied by some kicks indicating triggered emissions. During the D5 period there are a series of weak periodic emissions (indicated by arrows, ↓) in the range 5 to 7 kHz, which seem to be non-dispersive. In addition to these periodic emissions, there are very intense dispersive periodic emissions denoted by arrows (↑). The periods of dispersive and non-dispersive periodic emissions at 5 kHz are found to be exactly same. On the right half in D5 spectrogram in the range 4 to 5 kHz there seems to exist other periodic emissions probably with discrete structures.

3.3.2. Generation and propagation mechanism

The direction finding result has clearly demonstrated that the wave ducting is essentially important, giving rise to a strong wave-particle interaction where signal amplification takes place through phase bunching of the energetic electrons. The duct scale estimated by the DF is about 150 km in diameter, in good agreement with the previous satellite measurements by ANGERAMI (1970) and ONDOH (1976). During the early stage, we have observed multi-phased non-dispersive periodic emissions and during later stage the periodic emissions have changed from non-dispersive to dispersive. And in the D5 spectrogram we have received dispersive periodic emissions, which are coexisting simultaneously with the weak non-dispersive hiss bursts. On the whole, the frequency band occupied by the periodic emissions does not change so much during the event, that is, in the range 3 to 7 kHz. The parallel energy of resonant electrons is found to be 51 keV ($N=5\times10^2$ cm^{-3}) or 26 keV (10^3 cm^{-3}) for 3 kHz and 14 keV (5×10^2 cm^{-3}) and 7 keV (10^3 cm^{-3}) for 7 kHz. Finally this emission event may be closely associated with the onset of a substorm occurring about 6 hours before the emission event.

Dispersive periodic emissions are composed of a sequence of noise bursts, each of which is the result of whistler mode echoing of the previous burst. While in the case of non-dispersive periodic emissions, each burst appears in such a way that it is repeatedly triggered by another emission. The mechanism of no dispersion and dispersion in periodic emissions awaits future study.

3.4. Periodic emissions triggered by hiss emissions

During the observation there were some interesting triggered emissions. Fig. 11 illustrates two examples of those emissions. In the upper panel we see a well-defined, although weak, hiss band in 3 to 4 kHz, and also a sequence of dispersive periodic emissions with decreasing frequency (we can call each component "a slow faller"). They are given by arrows in the figure. The period at the upper end of each structure at 3.2 kHz is ~2.60 s. The detail of the fundamental component is such that $df/dt=0.56$ kHz/s in the range from 3.45 to 2.90 kHz and $df/dt=1.27$ kHz/s in 2.90 to 2.3 kHz. Similarly, the periodic emissions are triggered by the hiss band at ~4.2 kHz for the case of 4 November 1978 and each discrete structure takes

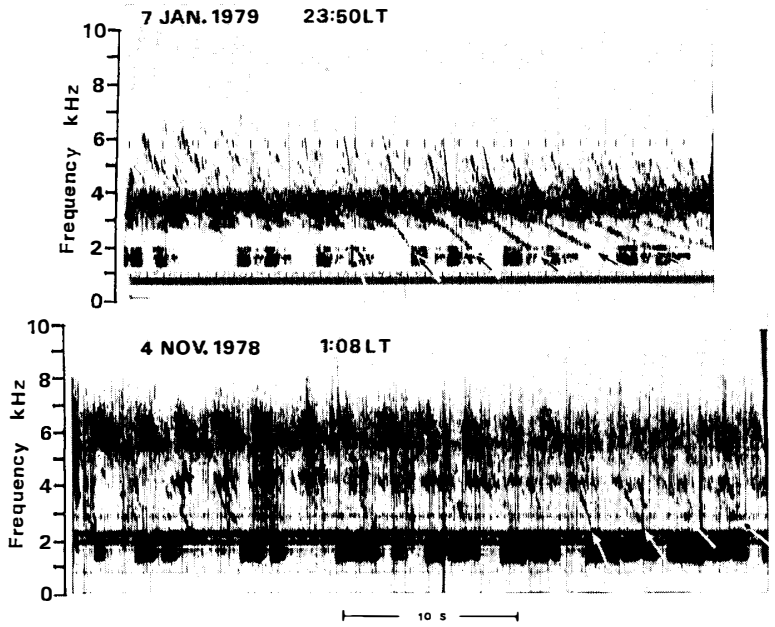

Fig. 11. Dispersive periodic VLF emissions triggered by the hiss band. The upper panel is from 7 January 1979, and the lower from 4 November 1978.

a form of a slow faller. The df/dt of the fundamental component is found to be $\sim$2.0 kHz/s.

4. Summary

We have shown only one example from each category of VLF emissions observed during our final year's campaign in Europe. By making use of the two different kinds of DF systems we were able to classify the emissions into several categories, and the DF results would be of great importance for the future detailed study of the generation and propagation mechanisms of each category of VLF/ELF emissions. In the study we will also make full use of the VLF data on board the satellites such as ISIS.

Acknowledgments

The present VLF/ELF research project was sponsored by the Japan Society for Promotion of Science, to whom we wish to express our sincere thanks. Thanks are also due to our co-investigators for this program; Drs. L. R. O. STOREY and C. BEGHIN of CRPE/CNRS at Orleans in France and Dr. T. S. JORGENSEN of Danish Meteorological Institute for their useful discussions. Finally we thank the staff of the

National Institute of Polar Research, who assisted us in analyzing some of our VLF data.

References

ANGERAMI, J. J. (1970): Whistler duct properties deduced from VLF observations made with the Ogo 3 satellite near the equator. J. Geophys. Res., **75**, 6115–6124.

ANGERAMI, J. J. and CARPENTER, D. L. (1966): Whistler studies of the plasmapause in the magnetosphere. 2. Electron density and total tube content near the knee in magnetospheric ionization. J. Geophys. Res., **71**, 711–725.

BULLOUGH, K., HUGHES, A. R. W. and KAISER, T. R. (1969): Satellite evidence for the generation of VLF emissions at medium latitudes by the transverse resonance instability. Planet. Space Sci., **17**, 363–374.

CARPENTER, D. L. and PARK, C. G. (1973): On what ionospheric workers should know about the plasmapause-plasmasphere? Rev. Geophys. Space Phys., **11**, 133–154.

FOSTER, J. C. and ROSENBERG, T. J. (1976): Electron precipitation and VLF emissions associated with cyclotron resonance interactions near the plasmapause. J. Geophys. Res., **81**, 2183–2192.

HAYAKAWA, M., TANAKA, Y. and OHTSU, J. (1975): On the morphologies of low-latitude and auroral VLF 'hiss'. J. Atmos. Terr. Phys., **37**, 517–529.

HAYAKAWA, M., BULLOUGH, K. and KAISER, T. R. (1977): Properties of storm-time magnetospheric VLF emissions as deduced from the Ariel 3 satellite and ground-based observations. Planet. Space Sci., **25**, 353–368.

HAYAKAWA, M., TANAKA, Y., OKADA, T. and IWAI, A. (1981): Goniometric direction finding for low-latitude whistlers. to be published in J. Geophys. Res., **86**.

MATHUR, A., RYCROFT, M. J. and SAGREDO, J. L. (1972): Ring current effect on magnetospheric electron density profiles derived from plasmapause whistlers. Nature, **237**, 508–510.

OKADA, T., HAYAKAWA, M. and IWAI, A. (1981): A new whistler direction finder. to be published in J. Atmos. Terr. Phys., **43**.

ONDOH, T. (1976): Magnetospheric whistler ducts observed by ISISsatellites. J. Radio Res. Labs., **23**, 139–147.

RYCROFT, M. J. (1972): VLF emissions in the magnetosphere. Radio Sci., **7**, 811–830.

TANAKA, Y., HAYAKAWA, M. and OHTSU, J. (1974): VLF hiss observed at a low-latitude ground station and its relation to drifting ring current electrons. Rep. Ionos. Space Res. Jpn, **28**, 168–172.

TANAKA, Y., HAYAKAWA, M. and NISHINO, M. (1976): Study of auroral VLF hiss observed at Syowa Station, Antarctica. Mem. Natl Inst. Polar Res., Ser. A (Aeronomy), **13**, 58 p.

(Received June 30, 1980; Revised manuscript received September 9, 1980)